Available online at www.sciencedirect.com
SCIENCE DIRECT®
Journal of the European Ceramic Society 25 (2005) 3055–3058
www.elsevier.com/locate/jeurceramsoc

# Evolution of low sigma grain boundaries in PTC thermistors during sintering

J. Seaton [1], C. Leach *

*Manchester Materials Science Centre, University of Manchester and UMIST, Grosvenor Street, Manchester M1 7HS, UK*

Available online 8 April 2005

**Abstract**

$BaTiO_3$-based positive temperature coefficient (PTC) thermistors undergo a large and rapid increase in grain boundary resistivity at temperatures just above the Curie temperature, $T_c$. Ample evidence exists for variability in the magnitude and form of the resistivity increase between different grain boundaries, and it has been noted that many of the grain boundaries showing a weak PTC effect have low $\Sigma$ values when indexed using coincidence site lattice notation. It has also been reported in the literature that, in undoped $BaTiO_3$, there is a strong preference for the formation of $\Sigma = 3$ grain boundaries in the microstructure, with many more present than would be expected by chance.

In the current study, the formation and retention of low $\Sigma$ grain boundaries in a PTC thermistor based on doped $BaTiO_3$ have been characterised through interrupted sintering experiments. Electron backscatter pattern (EBSP) analysis was used to establish grain boundary misorientation distributions in a series of samples prepared during an interrupted sintering study.

A significant proportion of $\Sigma = 3$, 5 and 9 boundaries was observed, with $\Sigma = 3$ boundaries being systematically preferred over other low $\Sigma$ boundaries. Since $\Sigma = 3$, 5 and 9 grain boundaries are believed to be PTC inactive, their presence in significant numbers in the microstructure is likely to be deleterious to the overall performance of a thermistor, particularly during transient loading.

An increase in the proportion of $\Sigma = 3$ twin boundaries was noted with sintering time, however, the proportion of $\Sigma = 3$ grain boundaries remained fairly constant, although occurring with a higher frequency than would be expected in a random population. The proportion of $\Sigma = 5$ and 9 boundaries also remained approximately constant during the sintering process, indicating that the density of low $\Sigma$ boundaries in the microstructure is fixed at an early stage of sintering and is not affected significantly by grain growth.


*Keywords:* Thermistors; $BaTiO_3$ and titanates; Grain boundaries; Interfaces; EBSP

## 1. Introduction

Positive temperature coefficient (PTC) of resistance thermistors, based on donor doped barium titanate, shows a large and rapid increase in grain boundary resistivity with increasing temperature. This occurs at temperatures just above the Curie temperature, $T_c$, and is associated with a ferroelectric to paraelectric phase transformation.[1] Early models for the PTC effect linked the increase in grain boundary resistivity to a sudden decrease in dielectric constant, which allowed an electrostatic barrier to develop.[1,2] These models were developed by considering the effects of spontaneous polarisation and by including the effect of secondary microstructural features such as grain boundary phases. More recently, the models have been refined further by incorporating the effects of charge shielding and trap activation.[3,4]

Studies of individual thermistor grain boundaries have shown that the magnitude of the PTC effect can differ widely between grain boundaries, with some grain boundaries showing large increases in resistance whilst others show little or no response.[5,6] Such differences in performance are generally attributed to variations in the amount of segregating dopants at different interfaces.[7] However, it has also been observed that the extent of PTC behaviour at a given grain boundary can be influenced by the geometry of the grain boundary and, in particular, the crystallographic misorientation across the interface. Using coincidence site lattice (CSL) notation, in which the value of $\Sigma$ that is ascribed to an

* Corresponding author. Tel.: +44 161 200 3561; fax: +44 161 200 3586.
*E-mail address:* colin.leach@man.ac.uk (C. Leach).
[1] Now at GE Thermometrics (UK) Ltd., Taunton.

0955-2219/$ – see front matter © 2005 Elsevier Ltd. All rights reserved.
doi:10.1016/j.jeurceramsoc.2005.03.189

interface is given by the reciprocal of the fraction of coincident atomic sites formed if the two lattices are overlapped,[8] several authors[9,10] have noted that $\Sigma = 3, 5$ and 9 grain boundaries characteristically exhibit little or no PTC effect, whereas randomly misoriented high-angle boundaries, not indexable as low $\Sigma$, tend to be associated with a large PTC resistivity increase.

A recent combined theoretical and experimental study of grain boundary misorientations in sintered untextured $BaTiO_3$ and $SrTiO_3$ revealed the presence of significantly more $\Sigma = 3$ grain boundaries in the sintered material than would be predicted within a population containing a random distribution of grain boundary misorientations.[11] If this were also to be the case in $BaTiO_3$ that has been processed to yield a PTC thermistor then the significant proportion of such grain boundaries, which are known to be electrically inactive, would have implications for device performance in the context of the local uniformity of electrical behaviour.

In this contribution, the results of a combined microstructural and crystallographic study to characterise the formation and retention of some low $\Sigma$ grain boundary types and structures during the sintering of a PTC thermistor are presented.

## 2. Experimental

The thermistor samples used in this study were prepared from donor doped $BaTiO_3$, containing additions of lead, strontium and calcium, by sintering at 1300 °C. A series of partially sintered pellets was prepared by quenching pellets after dwell times of between 0 and 60 min.

Polished faces of all of the pellets were prepared for microstructural analysis by grinding and polishing with progressively finer diamond pastes, down to 1 μm, and finishing with a colloidal silica solution to produce a strain-free surface finish suitable for EBSP analysis.

Microstructural characterisation was carried out using backscattered electron imaging and electron backscattered pattern (EBSP) analysis, using a Phillips XL30 FEGSEM equipped with an HKL EBSP analysis system. An in-house program[12] was used to establish the numbers and distributions of the chosen low $\Sigma$ interfaces.

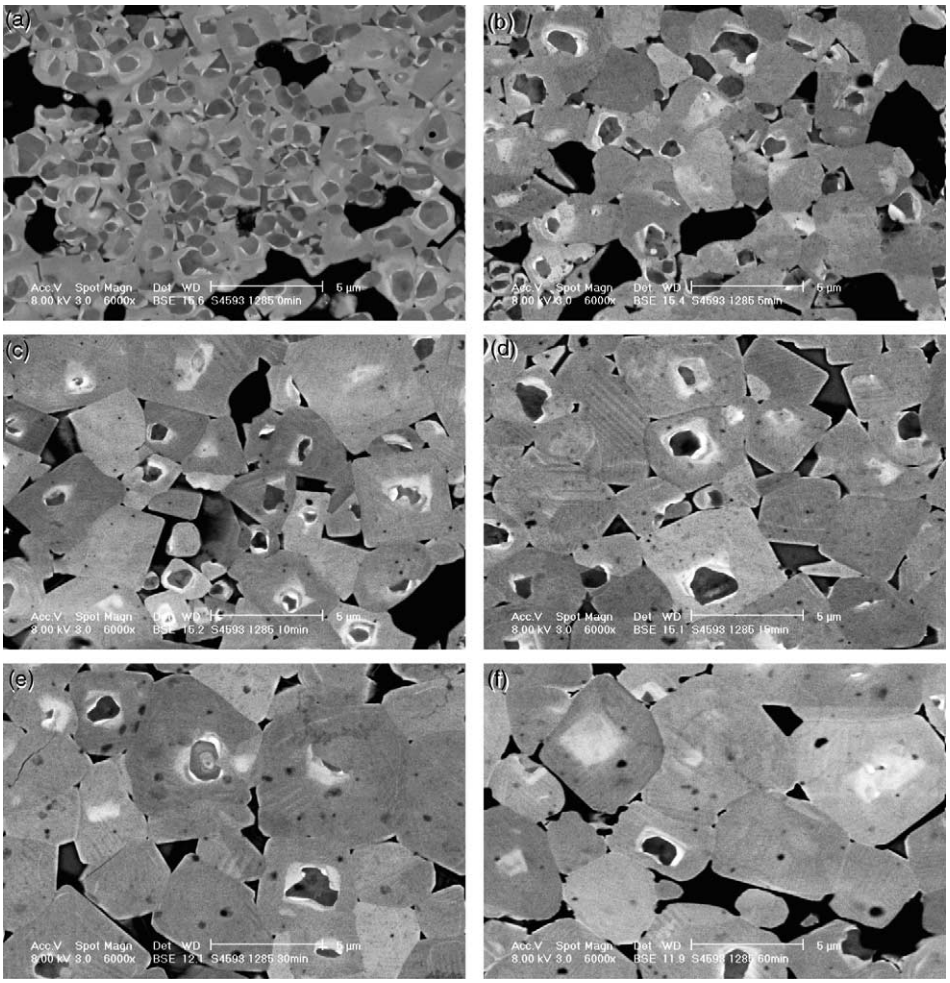


Fig. 1. Backscattered SEM images of the partially sintered samples after: (a) 0 min; (b) 5 min; (c) 10 min; (d) 15 min; (e) 30 min; and (f) 60 min dwell (scale bar = 5 μm).

## 3. Results and discussion

Fig. 1(a)–(f) shows the microstructures of the partially sintered samples. After 0 min dwell at the sintering temperature (Fig. 1(a)) densification has begun, but little grain growth has occurred, with the majority of grains ca. 1 μm in diameter. Porosity is distributed primarily at grain junctions and triple points. An inter-granular second phase is just visible, and is finely dispersed throughout the microstructure, in some cases surrounding individual grains.

After 5 min at the sintering temperature, some grain growth has begun (Fig. 1(b)), with grains up to 2.5 μm in diameter present. A secondary liquid phase is present and is most noticeable at triple points.

After 10 min at the sintering temperature, the morphology of the larger grains changes, as they start to become more regular in shape, showing a {1 0 0} habit with straight edges and square corners (Fig. 1(c)). A small number of the original grains remain, and both inter- and intra-granular porosity is present. The appearance of intra-granular porosity indicates that at this stage of sintering the drag force exerted by the pores on the grain boundaries has been overcome by the driving force for boundary motion, resulting in the pores becoming isolated in the grains.

After 15 min dwell grain growth, the pore size and second phase distribution are comparable with the fully sintered materials (Fig. 1(d)). The number of grains with a square habit has increased further, with the majority of grains now 4–5 μm in size.

With increasing dwell time, the smaller grains are eliminated and the final microstructure, comprising square, 4–5 μm grains with rounded corners, is approached (Fig. 1(e)–(f)). The level and form of porosity remain relatively constant during this period.

Density measurements from the central region of each interrupted sintering sample are shown in Fig. 2. When the sintering temperature is reached, the sample density is approximately 80% of theoretical, but after 15 min dwell, the density increases to ca. 95.5%, changing little thereafter.

EBSP analysis was carried out on the interrupted sintering samples to characterise the formation and retention of

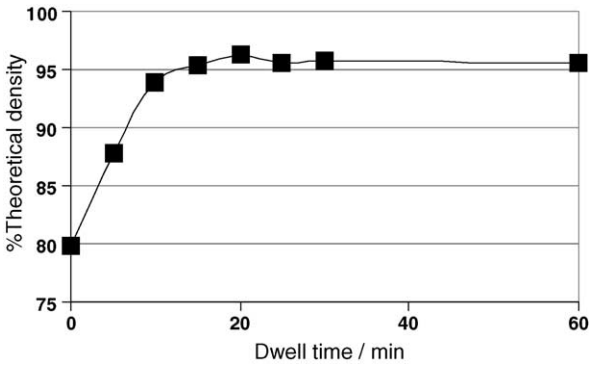


Fig. 2. Variation in sample density with sintering dwell time.

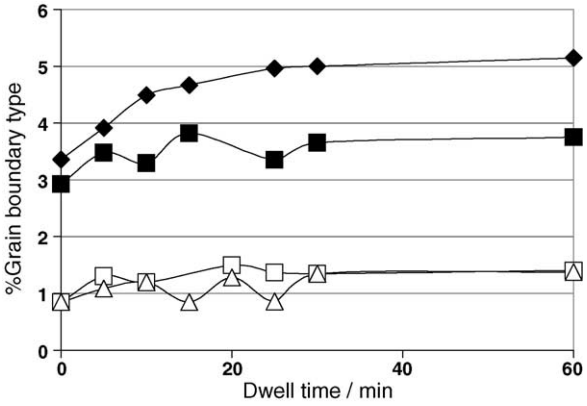


Fig. 3. Graph showing the variations in: $\Sigma = 3$ annealing twin (♦), $\Sigma = 3$ grain boundary (■), $\Sigma = 5$ grain boundary (□) and $\Sigma = 9$ grain boundary (△) populations with sintering time.

$\Sigma = 3$, 5 and 9 interfaces during sintering. Statistically significant data on the proportions of specific grain boundary types were collected by characterising a minimum of 300 grain boundaries within each sample. By observing the microstructure, it was possible to classify the $\Sigma = 3$ interfaces as either $\Sigma = 3$ annealing twins or $\Sigma = 3$ grain boundaries. Because of the limited penetration depth of backscattered electrons, all $\Sigma = 3$ twin boundaries, including those at a shallow angle to the surface, were able to be identified.

Fig. 3 shows the change in the percentage of $\Sigma = 3$ annealing twins and $\Sigma = 3$ grain boundaries in the microstructure with dwell time, along with variations on the proportion of $\Sigma = 5$ and 9 grain boundaries. It can be seen that the proportion of $\Sigma = 3$ grain boundaries in the microstructure remains approximately constant during sintering and grain growth, whilst there is a steady increase in the total number of $\Sigma = 3$ annealing twin interfaces up to a point where they account for 25% of the total $\Sigma = 3$ interface population. As with the $\Sigma = 3$ grain boundaries, the $\Sigma = 5$ and 9 grain boundaries show little change in their proportions as sintering proceeded. The $\Sigma = 3$ grain boundaries are present at about twice the expected level throughout the sintering process,[11] indicating that the

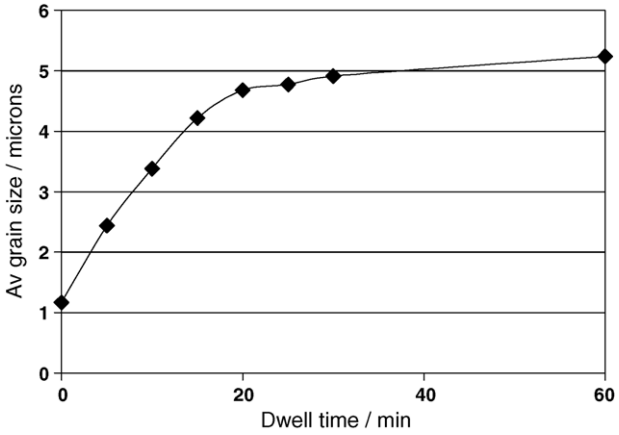


Fig. 4. Variation in sample grain size with sintering dwell time.

preferential formation and stabilisation of $\Sigma = 3$ grain boundaries in $BaTiO_3$ occurs at an early stage of sintering, and that these structures are retained during further densification and grain growth.

Fig. 4 shows a graph of mean grain size versus sintering time. The grain growth clearly follows the development of annealing twins within the microstructure, indicating that the proportion of grains containing annealing twins increases directly with the mean grain size. This suggests that the driving force for the formation of AT interfaces is a reduction in interfacial strain energy between neighbouring grains, rather than the overall minimisation of interfacial energy that is associated with grain growth.

## 4. Conclusions

An interrupted sintering study of a PTC thermistor indicated that maximum densification occurred after 15 min dwell time at the sintering temperature. Grain growth occurred inhomogeneously throughout the microstructure during sintering, although no anomalous grain growth was observed. EBSP analysis of a large number of grains allowed the misorientation of a statistically significant number of grain boundaries to be established. The proportion of $\Sigma = 3$ annealing twin interfaces increased during the first 30 min of sintering, while a relatively constant but higher than expected $\Sigma = 3$ grain boundary population was present throughout the sintering period. The proportions of $\Sigma = 5$ and 9 grain boundaries in the microstructure also remained largely unchanged during sintering, indicating that the final proportions of these low $\Sigma$ grain boundaries are established at an early stage of sintering and are not affected significantly by grain growth.

## References

1. Heywang, W., Resistivity anomaly in doped barium titanate. *J. Am. Ceram. Soc.*, 1964, **47**, 484–490.
2. Jonker, G. H., 'Advances in ceramics. 1. Grain boundary phenomena in electronic ceramics. *Am. Ceram. Soc.*, 1981, 155.
3. Gerthsen, P. and Hoffmann, B., Current–voltage characteristics and capacitance of single grain boundaries in semiconducting $BaTiO_3$ ceramics. *Sol. Stat. Elec.*, 1973, **16**, 617–622.
4. Miki, T., Fujimoto, A. and Jida, S., An evidence of trap activation for PTCR in $BaTiO_3$ ceramics with substitutional Nb and Mn as impurities. *J. Appl. Phys.*, 1998, **83**, 1592–1603.
5. Nemoto, H. and Oda, I., Direct examinations of PTC action of single grain. *J. Am. Ceram. Soc.*, 1980, **63**, 398–401.
6. Kuwabara, M., Morimo, K. and Matsunaga, T., Single-grain boundaries in PTC resistors. *J. Am. Ceram. Soc.*, 1996, **79**, 997–1001.
7. Desu, S. B. and Payne, D. A., Interfacial segregation in perovskites: IV, Internal boundary layer devices. *J. Am. Ceram. Soc.*, 1990, **73**, 3416–3421.
8. Randle, V., The role of the coincidence site lattice in grain boundary engineering. The Institute of Materials, 1996.
9. Ogawa, H., Demua, M., Yamamoto, T. and Sakuma, T., Estimation of the PTCR effect in single grain boundary of Nb-doped $BaTiO_3$. *J. Mater. Sci. Lett.*, 1995, **14**, 537–538.
10. Hayashi, K., Yamamoto, T. and Sakuma, T., Grain orientation dependence of the PTCR effect in niobium-doped barium titanate. *J. Am. Ceram. Soc.*, 1996, **79**, 1669–1672.
11. Ernst, F., Mulvihill, M. L., Kienzle, O. and Ruhle, M., Preferred grain orientation relationships in sintered perovskite ceramics. *J. Am. Ceram. Soc.*, 2001, **84**, 1885–1890.
12. Humphreys, F., VMAP analytical software, 1998–2004.